Synaptic input organization of the melanocortin system predicts diet-induced hypothalamic reactive gliosis and obesity

Tamas L. Horvath[a,b,c,1], Beatrix Sarman[a], Cristina García-Cáceres[d], Pablo J. Enriori[e], Peter Sotonyi[a], Marya Shanabrough[a], Erzsebet Borok[a], Jesus Argente[d], Julie A. Chowen[d], Diego Perez-Tilve[f], Paul T. Pfluger[f], Hella S. Brönneke[f,g], Barry E. Levin[h,i], Sabrina Diano[a,b,c], Michael A. Cowley[e,1], and Matthias H. Tschöp[f,1]

[a]Program in Integrative Cell Signaling and Neurobiology of Metabolism, Section of Comparative Medicine, Yale University School of Medicine, New Haven, CT 06520; [b]Department of Obstetrics/Gynecology and Reproductive Sciences, and [c]Department of Neurobiology, Yale University School of Medicine, New Haven, CT 06520; [d]Department of Endocrinology, Hospital Infantil Universitario Niño Jesús, Department of Pediatrics, Universidad Autónoma de Madrid, Los Centros de Investigación Biomédica en Red (CIBER) Fisiopatología Obesidad y Nutrición, Instituto de Salud Carlos III, E-28009 Madrid, Spain; [e]Department of Physiology, Monash University, Melbourne, VIC 3800, Australia; [f]Metabolic Diseases Institute, Division of Endocrinology, Department of Medicine, University of Cincinnati, Cincinnati, OH 45237; [g]German Institute of Human Nutrition Potsdam-Rehbrücke, 14558 Nuthetal, Germany; [h]Neurology Service, Department of Veterans Affairs New Jersey Health Care System, East Orange, NJ 07018; and [i]Department of Neurology and Neurosciences, New Jersey Medical School, University of Medicine and Dentistry of New Jersey, Newark, NJ 07101

Edited* by Jeffrey M. Friedman, The Rockefeller University, New York, NY, and approved July 6, 2010 (received for review March 30, 2010)

The neuronal circuits involved in the regulation of feeding behavior and energy expenditure are soft-wired, reflecting the relative activity of the postsynaptic neuronal system, including the anorexigenic proopiomelanocortin (POMC)-expressing cells of the arcuate nucleus. We analyzed the synaptic input organization of the melanocortin system in lean rats that were vulnerable (DIO) or resistant (DR) to diet-induced obesity. We found a distinct difference in the quantitative and qualitative synaptology of POMC cells between DIO and DR animals, with a significantly greater number of inhibitory inputs in the POMC neurons in DIO rats compared with DR rats. When exposed to a high-fat diet (HFD), the POMC cells of DIO animals lost synapses, whereas those of DR rats recruited connections. In both DIO rats and mice, the HFD-triggered loss of synapses on POMC neurons was associated with increased glial ensheathment of the POMC perikarya. The altered synaptic organization of HFD-fed animals promoted increased POMC tone and a decrease in the stimulatory connections onto the neighboring neuropeptide Y (NPY) cells. Exposure to HFD was associated with reactive gliosis, and this affected the structure of the blood-brain barrier such that the POMC and NPY cell bodies and dendrites became less accessible to blood vessels. Taken together, these data suggest that consumption of an HFD has a major impact on the cytoarchitecture of the arcuate nucleus in vulnerable subjects, with changes that might be irreversible due to reactive gliosis.

synaptic plasticity | brain | inflammation | vulnerability | high-fat diet

Efficient and safe pharmacologic options for the prevention and cure of obesity remain elusive. One reason for this failure is the incomplete understanding of the pathogenesis of obesity. A classic example of this is the lack of clarity regarding the molecular reasons why most individuals are prone, but some are resistant, to the obesogenic effects of a high-calorie diet. The currently favored model of molecular body weight control suggests that specific circuitry within the central nervous system (CNS) coordinates peripheral energy metabolism in response to constant input by environmental stimuli, circulating macronutrients, and afferent endocrine signaling (1).

Diet-induced obesity in rats recapitulates several features of human obesity, including the fact that obesity-prone (DIO) and -resistant (DR) types are inherited as polygenic traits that can arise from a single population (2–5). Because these rat models are indistinguishably lean before exposure to a high-fat diet (HFD), they can serve as suitable models for studying the pathogenesis of human obesity and the central nervous circuitry that regulates body adiposity (2–5).

The CNS melanocortin system is currently regarded as the *primum movens* of neuroendocrine body weight regulation (reviewed in refs. 1 and 6). Impaired melanocortin receptor signaling or insufficient availability of functional endogenous melanocortin agonists, which are derived from proopiomelanocortin (POMC)-expressing neurons of the hypothalamus, predisposes rodents and humans to development of DIO (7). Conversely, the targeted elimination of arcuate nucleus neurons that produce the MC4R inverse agonist AgRP, which normally provides a tonic inhibition of the POMC neurons, results in cessation of feeding, significant body weight loss, and death (8, 9). An insufficient stimulation of POMC neurons by afferent factors, such as leptin or insulin, is another cause of weakened CNS melanocortin tone and in some cases might contribute to the susceptibility to diet-induced obesity.

Beyond the regulation of AgRP and POMC neurons on a transcriptional level by leptin, ghrelin, and other afferent signals, circulating metabolic hormones can have a direct effect on these cells by altering neuronal firing, as demonstrated in vitro (10, 11). In addition, several lines of evidence have shown that the neuronal connectivity between specific populations of hypothalamic and extrahypothalamic neuronal systems implicated in the behavioral and endocrine regulation of energy balance is changing in response to metabolic hormones, such as leptin and ghrelin (12–18). In particular, the ratio of stimulatory and inhibitory inputs onto hypothalamic POMC neurons has been shown to be associated with the behavioral and endocrine effects of the melanocortin system to peripheral signals, as well as with the control of body weight in monogenetic models of obesity (reviewed in ref. 19). These observations led to formulation of the hypothesis that the input organization and plasticity of the melanocortin system is a significant determinant of metabolic phenotype (20). To investigate this possibility, we hypothesized that the qualitative and quantitative synaptic input organization of the POMC neurons would differ between animals that are vulnerable or resistant to the development of obesity even before their respective metabolic phenotype emerges, and, that the synaptic response to metabolic challenges would differ between

Author contributions: T.L.H., J.A.C., B.E.L., M.A.C., S.D., M.H.T., and P.J.E. designed research; T.L.H., B.S., C.G.-C., M.S., E.B., D.P.-T., P.T.P., H.S.B., M.A.C., S.D., M.H.T., P.S., P.J.E., and J.A. performed research; T.L.H., B.S., C.G.-C., M.S., J.A.C., D.P.-T., P.T.P., H.S.B., M.A.C., S.D., M.H.T., P.S., P.J.E., and J.A. analyzed data; and T.L.H. and M.H.T. wrote the paper.

The authors declare no conflict of interest.

*This Direct Submission article had a prearranged editor.

[1]To whom correspondence may be addressed. E-mail: tamas.horvath@yale.edu, michael.cowley@monash.edu, or matthias.tschoep@uc.edu.

NEUROSCIENCE

these groups. To examine whether the wiring of the melanocortin system could predict the vulnerability of animals to diet-induced obesity, we studied outbred Sprague–Dawley rats that were specifically developed to identify substrains that are either resistant or vulnerable to diet-induced obesity but are indistinguishable on a standard chow diet (SD) (2–5). We also investigated the same principal questions in C57bl6 mice maintained on either an SD or an HFD (21).

Results

DIO Rats Accrue More Fat Mass on Exposure to an HFD, but Do Not Differ From DR Rats Fed an SD. Body weight did not differ between the DIO rats and DR rats at the beginning of the study (Fig. 1*A*). Similarly, no significant differences in body weight were seen between the DIO and DR rats on an SD at the end of the study (Fig. 1*A*), indicating that the metabolism and adiposity of these two strains differ only and specifically in their response to a calorie-dense HFD. The body composition analysis by NMR demonstrated no difference in fat or lean mass between the DIO and DR rats on an SD (Fig. 1*B*). Consistent with numerous previous studies, the DIO rats gained significantly more body weight (Fig. 1*A*) and fat mass (Fig. 1*B*) during 12 wk of exposure to an HFD. As expected, plasma insulin and leptin levels increased, whereas circulating ghrelin levels decreased, with increasing adiposity (Fig. 1 *C*–*E*). Interestingly, hyperinsulinemia developed only in the DIO rats, although both the DIO and DR rats exhibited increased plasma levels of leptin on exposure to an HFD (Fig. 1 *C* and *D*); however, the rise in plasma leptin was considerably more pronounced in the DIO rats (Fig. 1*D*). Interestingly, ghrelin was lower in the DIO rats on an SD of equal body weight and body fat composition (Fig. 1*F*).

Synaptic Inputs of POMC Neurons of DIO and DR Rats. At the time when body weight and metabolic profile were similar in the DIO and DR rats on an SD, the POMC neurons of the DIO rats already had a greater number of synaptic connections compared with those of the DR rats ($P < 0.05$) (Fig. 2*A*). POMC perikarya of DR rats had the same numbers of asymmetrical (Fig. 2*B*) and symmetrical (Fig. 2*C*) synapses; however, those of DIO rates had significantly more symmetrical, inhibitory synapses than asymmetrical, excitatory contacts ($P < 0.05$) (Fig. 2*A*).

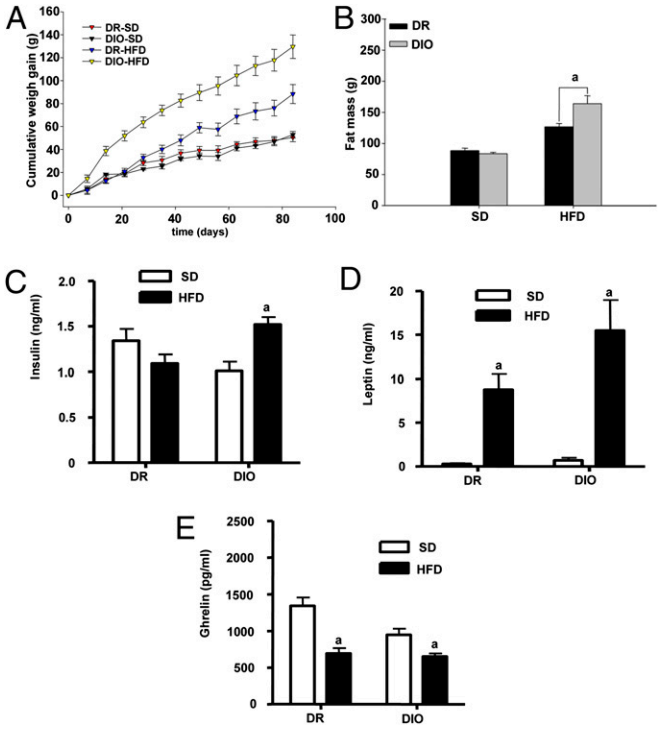

Fig. 1. The metabolic phenotype of DR and DIO rats fed an SD and those fed an HFD. (*A*) Body weight gain. (*B*) Fat mass. a: $P < 0.05$. (*C*) Insulin level. a: $P < 0.05$. (*D*) Leptin level. a: $P < 0.05$. (*E*) Total ghrelin level. a: $P < 0.05$. All results are mean ± SEM.

After 3 mo of exposure to an HFD, the density of synaptic connections on hypothalamic arcuate nucleus POMC neurons was changed in both DR and DIO rats. The DR rats on an HFD had an increased total number of synaptic connections onto POMC neurons compared with the DR animals on an SD ($P < 0.05$) (Fig. 2 *D* and *E*). In contrast, the total number of synapses on POMC neurons was lower in DIO mice on an HFD compared with those on an SD ($P < 0.05$) (Fig. 2 *D* and *F*). The number of asymmetrical, stimulatory inputs onto POMC neurons did not differ significantly in any of the four groups of rats that we evaluated (DIO on SD, DIO on HFD, DR on SD, and DR on HFD). The DIO rats on an SD had more inhibitory synaptic inputs onto the satiety-promoting POMC neurons compared with the DR rats on the same diet ($P < 0.05$) (Fig. 2*A*). This difference was reversed after 3 mo of an HFD; the perikarya of POMC neurons of the DR animals were dominated by symmetric, inhibitory connections, whereas those of the DIO rats were dominated by asymmetric, stimulatory contacts ($P < 0.05$) (Fig. 2*D*). This reversed constellation of synaptic input organization onto the POMC neurons was paradoxically associated with greaer body weight of the DIO animals compared with the DR rats (Fig. 1*A*). The NPY/AgRP perikarya could not be assessed in rats, because the labeling of NPY is limited to axonal processes. The total number of synapses on POMC neurons was increased in the DR animals ($P < 0.05$) (Fig. 2*G*), but decreased in the DIO rats ($P < 0.05$) (Fig. 2*G*).

Astroglia in DR and DIO Rats. In HFD-fed DIO rats, in which POMC perikarya had a lower number of synapses, there was an increased appearance of glial ensheathment of the plasma membrane of the melanocortin cells (Fig. 2*F*). The DIO animals had a higher level of astrocytic coverage ($P < 0.001$) on the POMC cells compared with the DR animals (39.46 ± 5.67 μm/100 μm vs. 22.84 ± 2.74 μm/100 μm perikaryal membrane of POMC cells) (Fig. 2*H*).

Synaptic Input Organization of the Melanocortin System in SD- and HFD-Fed Mice. We analyzed the synaptic input organization of NPY/AgRP and POMC neurons from cohorts of GFP-NPY and GFP-POMC mice (C57Bl6; ref. 12) on an SD or an HFD. The metabolic parameters of these models have been reported previously (21). In brief, they became obese, hyperleptinemic, leptin-resisitant, and insulin-resistant after 20 wk of an ad libitum HFD (21). Mice fed an SD for 20 wk remain lean and leptin- and insulin-sensitive (21). We found that both POMC and NPY neurons had fewer synapses on their perikarya in the mice fed an HFD ($P < 0.05$ vs. SD) (Fig. 3 *A* and *B*). However, the decrease in total numbers of synapses on POMC perikarya affected inhibitory, symmetric contacts only (Fig. 3*A*), whereas the loss on NPY perikarya was associated with stimulatory, asymmetric contacts (Fig. 3*B*). Thus, the synaptic input organization of the POMC neurons was similar in mice fed an HFD and DIO rats, suggesting a decreased inhibitory tone triggered by HFD-induced synaptic plasticity. On the other hand, NPY neurons exhibited decreased excitatory input after HFD exposure, suggesting decreased activity of these cells.

Glial Cells in the Hypothalamus of SD- and HFD-Fed Mice. Similar to our observations in rats, the HFD induced a robust induction of GFAP-immunolabeled astrocytic profiles in the arcuate nucleus (Fig. 3 *C* and *D*). There was an increased presence of glial processes around GFP-positive perikarya. Glial ensheathment of both POMC and NPY cells was significantly elevated in the HFD-fed

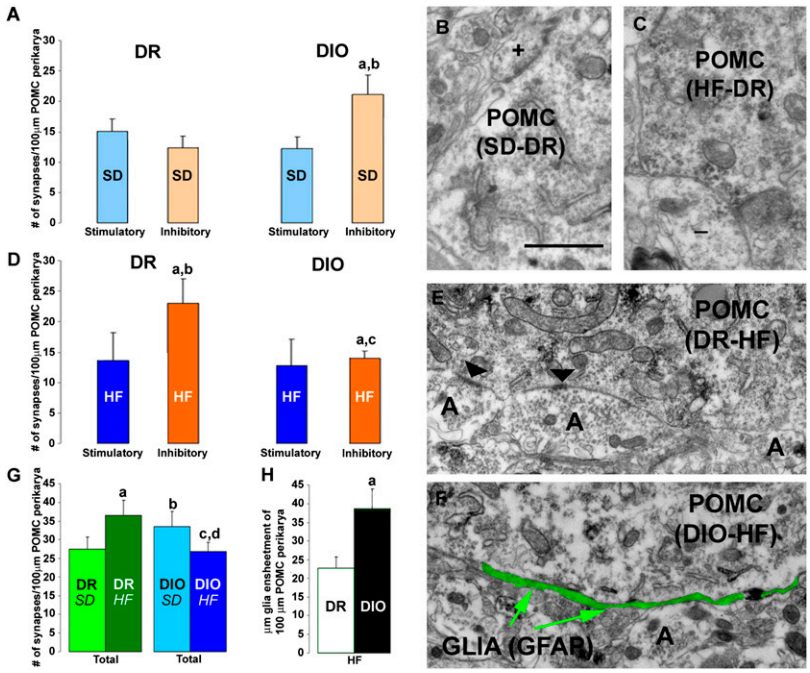

Fig. 2. Synaptic input organization of DR and DIO rats. (*A*) Bar graphs showing the numbers of perikaryal symmetrical and asymmetrical connections on POMC neurons of DR and DIO animals fed an SD. a and b: $P < 0.05$. (*B* and *C*) Representative electron micrographs showing asymmetrical, putative stimulatory (+; *B*), and, symmetrical, putative inhibitory (–; *C*) synapses taken from POMC-immunolabeled perikarya of an SD-fed DR rat (*B*) and of an SD-fed DIO rat (*C*). (Scale bar in *B*: 1 μm for *B*, *C*, *E*, and *F*.) (*D*) Bar graphs showing the numbers of perikaryal symmetrical and asymmetrical connections on POMC neurons of DR and DIO animals fed an HFD. (*E* and *F*) Representative electron micrographs showing POMC-labeled perikarya of a DR HFD mouse (*E*) and a DIO HFD mouse (*F*). Note that instead of the axon terminals (A) in the DR HFD POMC cells, there is glial ensheathment (indicated by green pseudocolor) of the POMC perikarya of the DIO HFD animal. Bar graphs represent mean ± SEM. (*G*) Bar graph indicating the total numbers of synapses on POMC perikarya of DR and DIO rats fed an SD and an HFD. a: $P < 0.05$ DR HFD versus DR SD; b: $P < 0.05$ DIO SD versus DR SD; c: $P < 0.05$ DIO HFD versus DIO SD. (*H*) Bar graphs indicating glial ensheathment on POMC perikarya of DR and DIO animals fed an HFD. a: $P < 0.05$.

mice compared with SD-fed animals (POMC: 0.363 ± 0.02 vs. 0.246 ± 0.03 μm/100 μm perikaryal membrane of GFP-POMC cells, $P < 0.05$; NPY: 0.347 ± 0.018 vs. 0.23 ± 0.04 μm/100 μm perikaryal membrane of GFP-NPY cells, $P < 0.05$). Strikingly, when analyzed by electron microscopy, a dramatic difference also emerged regarding the close proximity of POMC and NPY neurons to capillaries of the arcuate nucleus (Fig. 3 *D*–*G*). In animals on an SD, close appositions between POMC (Fig. 3*D*) and NPY perikarya and vessels of the arcuate nucleus parenchyma were common. Within these close appositions, neuronal profiles were separated from the endothelial cells of the vessels by a thin layer of glia (glia endfeet; Fig. 3*D*, *Inset*). These types of physical relationships between perikarya or dendrites of the melanocortin system (either NPY or POMC neurons) were not observed in HFD-fed, obese animals (Fig. 3 *F* and *G*). For 25 encounters of close apposition between either GFP-NPY or GFP-POMC cells and the glia endfeet of vessels in SD-fed animals ($n = 4$), no such interactions were seen in HFD-fed animals ($n = 4$) ($P < 0.00001$).

Subsequently, we quantified capillaries in the arcuate nucleus of mice fed an SD or an HFD. We analyzed the same arcuate nucleus region as for synaptic counts and neuron–vessel interactions. We found no statistical difference in the number of capillaries between SD-fed mice ($n = 5$) and HFD-fed mice ($n = 5$) (16.66 ± 1.46/400 μm vs. 12.25 ± 2.25/400 μm; $P = 0.181$) (Fig. 4 *A* and *B*). Conversely, the mean capillary diameter was significantly greater in the HFD-fed mice ($n = 5$) compared with the SD-fed mice ($n = 5$) (14.69 ± 1.4 μm vs. 8.97 ± 0.6 μm; $P = 0.0002$) (Fig. 4 *C* and *D*).

Hypothalamic Expression of GFAP, POMC, and NPY mRNA in SD- and HFD-Fed Mice. Given the observed changes in glia and synaptic input organization onto the NPY/AgRP and POMC neurons, we analyzed the transcript levels of GFAP, NPY and POMC in arcuate nuclei of mice placed on HFD at 60 d of age or maintained on SD (Fig. 4 *E*–*G*). There was a significant effect of HFD on NPY, POMC, and GFAP mRNA levels (GFAP: $F = 6.291$, $P < 0.03$; POMC: $F = 8.067$, $P < 0.02$; NPY: $F = 12.974$, $P < 0.002$). Animals fed an HFD during adulthood had increased GFAP and POMC mRNA levels but decreased NPY mRNA levels in the arcuate nucleus compared with their SD-fed littermate controls (Fig. 4 *E*–*G*).

Discussion

Intense efforts are being devoted to improving our understanding of the molecular mechanisms of energy balance regulation. These endeavors have already led to the identification of numerous new pathways involved in the control of body weight. However, the exact molecular reasons for the distinction between the widespread susceptibility to diet-induced obesity and the much less frequent resistance to this most common form of obesity remain unknown. Although models of monogenetic obesity, such as the leptin-deficient ob/ob mouse, have provided important insights into single pathways (22), their value in increasing our understanding of diet-induced obesity has proven to be limited. Polygenic models such as the DIO and DR rats and mice may represent a better surrogate model for the human disease, more suitable to dissect its pathogenesis and study its consequences. One particularly valuable feature of these models is that they allow for a comparison between obesity-resistant and obesity-prone animals in a preobese state. Several differences in traits and characteristics between DIO rats and DR animals of equal body adiposity before exposure to an HFD have been reported (2–5); however, no synaptologic correlate has yet been identified that can help explain the differences between DIO and DR rats in terms of their susceptibility to diet-induced obesity.

Our results show that rats with high susceptibility to DIO exhibit significant and typical differences in the wiring of their POMC neurons compared with DR animals with comparable metabolic characteristics while fed an SD. The synaptic input organization of lean DIO rats favors an increased inhibitory tone on their POMC neurons compared with the pattern seen in DR rats. This constellation of neural connections is in line with the increased vulnerability of DIO animals to weight gain when fed an HFD. However, once exposed to an HFD, POMC neurons of DIO and DR rats exhibit diametrically different development of synaptic plasticity. This is reflected by the decreased number of connections but increased number of excitatory contacts in the DIO POMC (anorexigenic) neurons, whereas the DR POMC neurons actually gain connections with mostly new inhibitory contacts. Thus, whereas the wiring of POMC neurons while on an SD accurately predicts vulnerability to weight gain on HFD, the synaptic input organization of POMC neurons after exposure to an HFD is

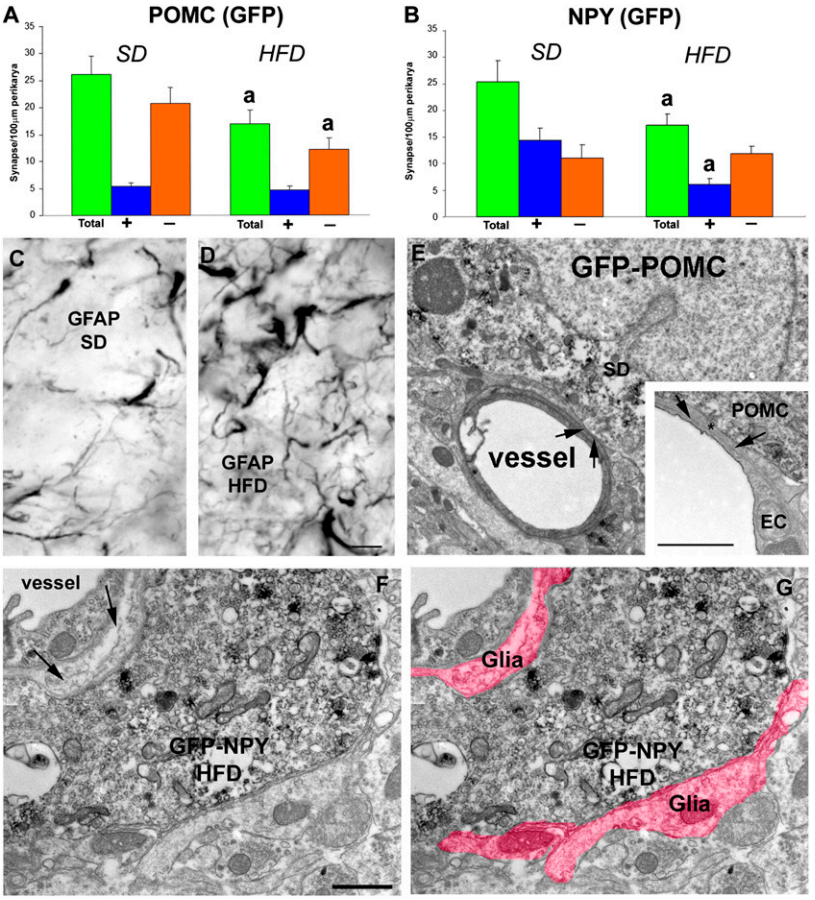

Fig. 3. Synaptology of arcuate nucleus NPY and POMC neurons from SD- and HFD-fed DIO mice. (*A* and *B*) Bar graphs showing total, inhibitory, and excitatory synapses on POMC (*A*) and NPY (*B*) neurons from animals fed an SD and those fed an HFD. a: $P < 0.05$ HFD versus SD values. (*C* and *D*) Representative light micrographs showing GFAP immunolabeling in the arcuate nucleus of animals fed an SD (*C*) or an HFD (*D*). (Scale bar in *E*: 10 μm for *C* and *D*.) (*E*) Electron micrograph of a typical direct apposition between a POMC perikaryon and a vessel in SD-fed mice. (*Inset*) Higher-power magnification of a contact between a POMC perikaryon and the glia limitans of a vessel. The star indicates the space between the POMC perykaryon and the endothelial cell of a vessel. Arrows point to the thin layer of glia. (Scale bar: 1 μm.) (*F* and *G*) The same electron micrograph of a GFP-NPY perikaryon from a HFD-fed animal in the vicinity of a vessel in the arcuate nucleus. Note the increased presence of glia between the vessel and the labeled perikaryon (arrows in *F*) and other parts of the cell body. The pseudocolor in *G* indicates glial processes around the labeled NPY cell. (Scale bar in F: 1 μm for *F* and *G*.) Bar graphs represent mean ± SEM.

not in line with the metabolic phenotype of DIO and DR rats. This might be a manifestation of physiological compensation efforts in an attempt to promote POMC tone in DIO animals.

We also found that in mice, HFD-induced obesity is associated with synaptic reorganization of the arcuate nucleus melanocortin system. Both POMC and NPY neurons had fewer total synapses on their perikarya in HFD-fed mice; however, the loss of synapses on POMC perikarya affected inhibitory, symmetric contacts, whereas the loss of synapses on NPY perikarya was associated with stimulatory, asymmetric contacts. The apparent specificity in the alteration of the inhibitory contacts on POMC cells differs between mice and rats. (Because of technical limitations, NPY perikarya could not be analyzed specifically in rats.) Nevertheless, the trend toward a decreased overall inhibitory tone on the POMC cells is consistent in both species and experimental animal models. In both the rat and mouse studies, an induction in the number of astrocytic profiles (reactive gliosis) occurred that took the place of synapses on perikaryal membranes and "filled the space" between cells and vessels in response to an HFD.

Reactive gliosis is a hallmark of inflammation (23). An understanding of how this inflammatory gliosis emerges in the arcuate nucleus will be of critical relevance for an improved understanding of the etiology of metabolic dysfunctions associated with high-fat, high-calorie intake. We suggest that multiple events might propagate reactive gliosis in the arcuate nucleus. First, because of repeated daily cycles of synaptic plasticity associated with changing peripheral metabolism and hormone levels (20), glial cells are continuously engaged in elevated activity, which in turn may lead to increased cellular stress. Second, leptin and other afferent factors may directly target glial cells (24, 25) and promote glial proliferation and GFAP expression. This possibility is further supported by the finding that selective knockout of Stat-3, a critical downstream effector of leptin signaling, from glial cells, diminishes the induction of reactive gliosis and GFAP in response to stress (26). Third, satiety promoted by leptin triggers reactive oxygen species generated by POMC neurons (18), which consequently may contribute to the initiation of reactive gliosis. The idea that POMC neurons may actually be very active during HFD exposure also may be inferred from our synaptology studies; POMC neurons from HFD-fed animals showed a highly similar trend toward a decreased inhibitory tone on the perikarya in rats and mice. On the other hand, NPY/AgRP neurons of HFD-fed mice exhibited reduced excitatory input, suggesting a decreased level of activity on their part. The mRNA levels of these transcripts (NPY and POMC) confirm the probability that of increased activity of the POMC neurons and decreased activity of the NPY cells, with increased GFAP transcript in association with increased astrocyte numbers and/or processes.

Taken together, our data appear to reveal a striking paradox, with the wiring of the melanocortin system of vulnerable animals in response to a hypercaloric environment reflecting an adequate, possibly maximal, responsiveness of these cells to leptin. This is surprising in view of the current model that suggests that these animals should be in a state of systemic leptin resistance. Consistent with this conclusion from our current observations is the fact that the synaptic input organization of POMC neurons on an HFD with elevated leptin levels shows a similar trend of changes as those that we described previously for highly sensitive ob/ob mice in response to leptin administration (12). It is also apparent that the gliosis that we report here in response to an HFD might not be the cause of leptin resistance as was proposed earlier (27), because despite the increased glial presence around vessels, POMC neuronal wiring is essentially as expected in re-

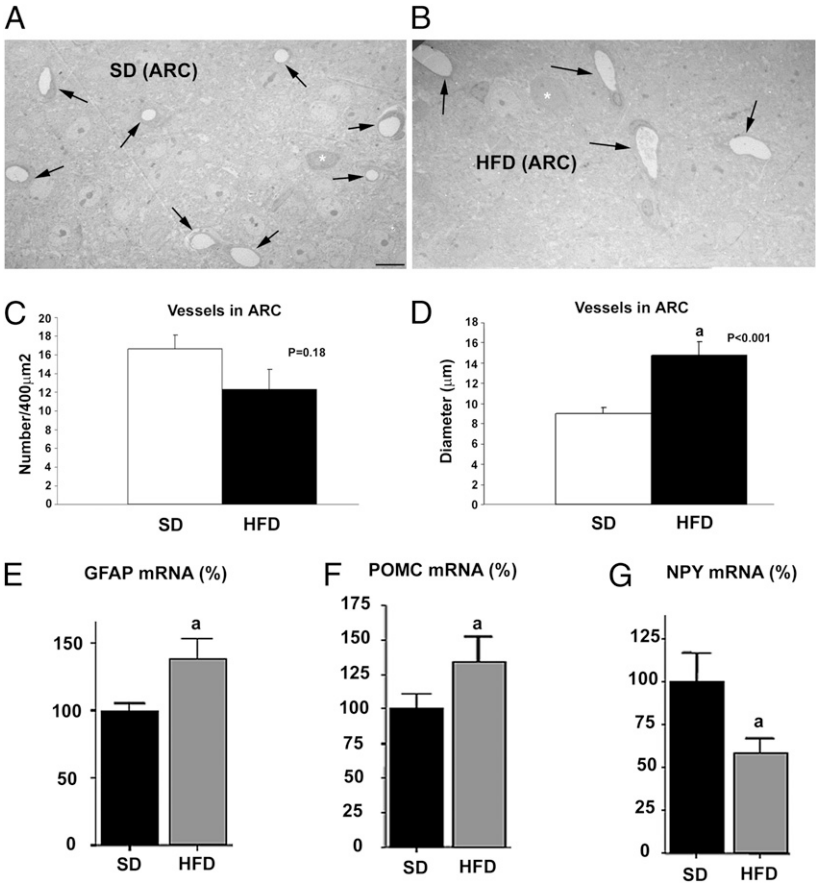

Fig. 4. Capillaries and arcuate nucleus transcript levels of GFAP, POMC, and NPY from mice fed an SD and an HFD. (*A* and *B*) Low-power magnification electron micrographs showing capillaries (black arrows) in the arcuate nucleus from an animal fed an SD (*A*) and an animal fed an HFD (*B*). (Scale bar in *A*: 10 μm for *A* and *B*.) (*C*) Bar graphs showing no statistically significant differences in numbers of capillaries between the two groups. (*D*) Bar graph showing that the diameter of capillary lumen is greater in the arcuate nucleus of animals fed an HFD compared with animals fed an SD. (*E*) Graph showing an increased level of GFAP mRNA in the arcuate nucleus of HFD-fed mice compared with SD-fed lean control mice (a: $P < 0.05$). (*F*) Graph showing an increased level of POMC mRNA in the arcuate nucleus of HFD-fed mice compared with SD-fed lean controls (a: $P < 0.05$). (*G*) Graph showing a decreased level of NPY mRNA in the arcuate nucleus of HFD-fed DIO mice compared with SD-fed lean controls (a: $P < 0.05$). Bar graphs represent mean ± SEM.

sponse to strong leptin input. It is also conceivable that assays using hypothalamic slices to measure α-MSH release (21) might be skewed by gliosis, an event that may provide a structural obstacle for leptin to reach neurons and/or for the release of α-MSH into the medium, and thus these assays might be of limited value for the study of α-MSH release kinetics. In fact, the explanation for decreased occupancy of MC4Rs on an HFD does not have to originate from decreased secretory activity of POMC neurons; a recent study unmasked the existence of a prolylcarboxypeptidase (PRCP), which potently inactivates extracellular α-MSH and is expressed in hypothalamic sites where α-MSH is released with high affinity to inactivating α-MSH (28), offering an alternate mechanistic explanation. At the same time, the recent results on the role of Toll-like receptor and JNK signaling in promoting leptin resistance (29, 30) mandate further investigations into the roles of various intracellular elements of inflammation in the etiology of hypothalamic dysfunctions.

While the central integration of afferent signals reflecting acute and chronic energy requirements becomes clearer, the neuronal pathways that actually initiate changes in body adiposity remain largely unknown, as does our understanding of how their numerous intraneuronal signaling modalities fine-tune energy balance regulation. Base wiring and the "flexibility" of synaptic plasticity are concepts with the potential to shed new light on the mechanism of the central regulation of body weight and offer explanations as to why no suitable pharmacologic cure for obesity has yet been developed. Although it is established that changes in hypothalamic synaptic plasticity of satiety-promoting melanocortin neurons can be triggered by afferent (energy balance–regulating) hormones such as leptin, estradiol, and ghrelin (12, 16), it is almost certain that the individual variability of wiring and overall flexibility of these circuits originate developmentally due to complex patterns of genetic, epigenetic, and environmental pressures (31–35).

Materials and Methods

Animals. ***Rats.*** Adult male (7 mo old at the start of the study) DIO and DR rats [outbred Sprague–Dawley rats selectively bred for high (DIO) and low (DR) weight gainers] (2) were housed singly in an environmental temperature of 22 °C with a 12:12-h light-dark cycle (lights on at 6:00 AM) in type III Makrolon cages with soft wood bedding. Six body weigh- and age-matched rats were included in each study group (DIO-SD, DIO-HFD, DR-SD, and DR-HFD). Animals were exposed for 3 mo to either an SD or an HFD (Altromin). The SD (maintenance diet for rats and mice) contained 4% fat, 50.5% carbohydrates, and 19% protein (wt/wt), with 13%, 63%, and 24% of total digestible energy (11.8 kJ/g) from fat, carbohydrates, and protein, respectively. The HFD (art. no. C1057) contained 15% fat, 47% carbohydrates, and 17% protein (wt/wt), with 34%, 48%, and 17% of total digestible energy (16.2 kJ/g) from fat, carbohydrates, and protein, respectively. Food and water were available ad libitum. Body weight was measured once weekly. Body composition was measured in all rats using NMR technology (EchoMRI; Echo Medical Systems). Measurements were performed in all rats after 3 mo of exposure to either the SD or the HFD. The animals were maintained in accordance with National Institutes of Health guidelines for the care and use of laboratory animals, and all experiments were approved by the Ethics Committee of the State Ministry of Agriculture, Nutrition, and Forestry, Brandenburg, Germany.

Immunoassays. Plasma leptin and insulin levels were quantified using a Luminex Multiplex Analyzer and compatible Lincoplex immunoassays in one simultaneous multipanel assay (Linco-Millipore). Total plasma ghrelin levels were measured using a well-established commercially available RIA (Phoenix Peptides).

Mice. The synaptic input organization of NPY and POMC neurons was analyzed in mice resistant or sensitive to diet-induced obesity. The metabolic phenotype of these animals was reported by Enriori et al. (21). We used the brains of the mice described in that study and from a study that we carried out using a similar approach. In brief, at 6 wk of age, C57BL/6J mice (Jackson

Laboratory) crossed with GFP-NPY (backcrossed seven generations onto C57BL) and GFP-POMC (conjenic C57 Bl6) animals were fed a, SD (Purina Lab Chow #5001; Ralston Purina) or an HFD (Rodent Chow #D12451; Research Diets) for 20 or 37 wk. The SD provided 3.3 kcal/g of energy (59.8% carbohydrate, 28.0% protein, and 12.1% fat). The HFD provided 4.75 kcal/g of energy (35.0% carbohydrate, 20.0% protein, and 45.0% fat). Mice were housed (five per cage) in a controlled environment, and body weight was measured weekly. Food and water were available ad libitum unless indicated otherwise. Mouse procedures were performed in accordance with the guidelines and approval of the Oregon National Primate Research Center's Institutional Animal Care and Use Committee. Body composition was measured by dual X-ray absorbiometry (Lunar Piximus; GE Medical Systems). As reported by Enriori et al. (21), a cohort of animals on the HFD developed obesity, gaining 30% more weight than their SD controls (DIO mice) during 20 wk on the diet, whereas another cohort of animals gained only around 6% compared with the SD controls (DR mice). We compared the synaptology of NPY and POMC neurons of mice at 20 wk after SD or HFD exposure. We also quantified the number of capillaries and their diameter in the same material. Random electron microscopy sections from anterior, middle, and posterior regions of the arcuate nucleus were photographed at 813× magnification from each animal in the SD (n = 5) and HFD groups (n = 5). Capillaries were counted and their diameters recorded digitally.

Brain Preparation and Electron Microscopy. The animals were perfused with paraformaldehyde fixative, and their brains were processed for immunolabeling for POMC (rats) or GFP (mice) for electron microscopy examination. Ultrathin sections were cut on a Leica ultra-microtome, collected on Formvar-coated single-slot grids, and analyzed with a Tecnai 12 Biotwin electron microscope (FEI). The analysis of synapse number was performed in an unbiased fashion as described elsewhere (12, 13, 15–18). Nonparametric ANOVA was used for multiple statistical comparisons. The Mann-Whitney U test was used to determine the significance of differences between groups. The statistical confidence was set at $P < 0.05$.

Real-Time PCR. Animals fed an HFD and those fed an SD were used for these analyses. Hypothalami were rapidly collected and snap-frozen in liquid nitrogen at 3 h after ghrelin or saline injection. Total RNA was extracted using TRIzol (Invitrogen) following the manufacturer's instructions. cDNA was synthesized using the First-Strand cDNA Kit (Amersham) following the manufacturer's instructions. Real-time PCR was performed with SYBR Green (BioRad) using specific primers for NPY, POMC, or GFAP. Reaction products were confirmed by sequencing of selected samples.

Quantification of Astrocytic Coverage on NPY and POMC Cells. The analysis of the astrocytic coverage of the cell membrane of labeled POMC cells (rats and mice) and NPY neurons (mice) was performed using ImageJ. Electron microscopy photographs (11,500×) were used to first measure the perimeter of each POMC cell analyzed, followed by determination of the amount of membrane covered by astrocytes (in nanometers). The results are reported as astrocyte coverage/perimeter of the POMC.

Statistical Analysis. Statistical analyses were performed using SPSS version 13.0. All data are presented as mean ± SEM. To determine if there was an interaction between experimental groups, two-way ANOVAs was performed. Post hoc comparisons were made using the Bonferroni´s test. Values were considered significantly different at $P < 0.05$.

ACKNOWLEDGMENTS. We are indebted to Ms. Anne Evans for her excellent technical support. Studies described in this paper were supported by National Institutes of Health (NIH) Grants DK 080000 and DK 060711 and American Diabetes Association (ADA) Grant 7-08-MN-25 (to T.L.H.), ADA Grant 1-08-RA-36 (to S.D.), NIH Grants RR 0163 and DK 62202 (to M.A.C.), and NIH Grants DK 056863 and DK 077975 (to M.H.T.).

1. Gao Q, Horvath TL (2007) Neurobiology of feeding and energy expenditure. *Annu Rev Neurosci* 30:367–398.
2. Levin BE, Dunn-Meynell AA, Balkan B, Keesey RE (1997) Selective breeding for diet-induced obesity and resistance in Sprague–Dawley rats. *Am J Physiol* 273:R725–R730.
3. Levin BE, Keesey RE (1998) Defense of differing body weight set points in diet-induced obese and resistant rats. *Am J Physiol* 274:R412–R419.
4. Levin BE, Dunn-Meynell AA (2000) Defense of body weight against chronic caloric restriction in obesity-prone and -resistant rats. *Am J Physiol Regul Integr Comp Physiol* 278:R231–R237.
5. Levin BE, et al. (2003) A new obesity-prone, glucose-intolerant rat strain (F.DIO). *Am J Physiol Regul Integr Comp Physiol* 285:R1184–R1191.
6. Cone RD (2006) Studies on the physiological functions of the melanocortin system. *Endocr Rev* 27:736–749.
7. Farooqi IS, et al. (2003) Clinical spectrum of obesity and mutations in the melanocortin 4 receptor gene. *N Engl J Med* 348:1085–1095.
8. Gropp E, et al. (2005) Agouti-related peptide-expressing neurons are mandatory for feeding. *Nat Neurosci* 8:1289–1291.
9. Luquet S, Perez FA, Hnasko TS, Palmiter RD (2005) NPY/AgRP neurons are essential for feeding in adult mice but can be ablated in neonates. *Science* 310:683–685.
10. Cowley MA, et al. (2001) Leptin activates anorexigenic POMC neurons through a neural network in the arcuate nucleus. *Nature* 411:480–484.
11. Cowley MA, et al. (2003) The distribution and mechanism of action of ghrelin in the CNS demonstrates a novel hypothalamic circuit regulating energy homeostasis. *Neuron* 37:649–661.
12. Pinto S, et al. (2004) Rapid rewiring of arcuate nucleus feeding circuits by leptin. *Science* 304:110–115.
13. Horvath TL, Gao XB (2005) Input organization and plasticity of hypocretin neurons: Possible clues to obesity's association with insomnia. *Cell Metab* 1:279–286.
14. Sternson SM, Shepherd GM, Friedman JM (2005) Topographic mapping of VMH → arcuate nucleus microcircuits and their reorganization by fasting. *Nat Neurosci* 8: 1356–1363.
15. Diano S, et al. (2006) Ghrelin controls hippocampal spine synapse density and memory performance. *Nat Neurosci* 9:381–388.
16. Abizaid A, et al. (2006) Ghrelin modulates the activity and synaptic input organization of midbrain dopamine neurons while promoting appetite. *J Clin Invest* 116:3229–3239.
17. Gao Q, et al. (2007) Anorectic estrogen mimics leptin's effect on the rewiring of melanocortin cells and Stat3 signaling in obese animals. *Nat Med* 13:89–94.
18. Andrews ZB, et al. (2008) UCP2 mediates ghrelin's action on NPY/AgRP neurons by lowering free radicals. *Nature* 454:846–851.
19. Horvath TL, Diano S (2004) The floating blueprint of hypothalamic feeding circuits. *Nat Rev Neurosci* 5:662–667.
20. Horvath TL (2005) The hardship of obesity: A soft-wired hypothalamus. *Nat Neurosci* 8:561–565.
21. Enriori PJ, et al. (2007) Diet-induced obesity causes severe but reversible leptin resistance in arcuate melanocortin neurons. *Cell Metab* 5:181–194.
22. Zhang Y, et al. (1994) Positional cloning of the mouse obese gene and its human homologue. *Nature* 372:425–432.
23. Norton WT, Aquino DA, Hozumi I, Chiu FC, Brosnan CF (1992) Quantitative aspects of reactive gliosis: A review. *Neurochem Res* 17:877–885.
24. Diano S, Kalra SP, Horvath TL (1998) Leptin receptor immunoreactivity is associated with the Golgi apparatus of hypothalamic neurons and glial cells. *J Neuroendocrinol* 10:647–650.
25. Hsuchou H, et al. (2009) Obesity induces functional astrocytic leptin receptors in hypothalamus. *Brain* 132:889–902.
26. Herrmann JE, et al. (2008) STAT3 is a critical regulator of astrogliosis and scar formation after spinal cord injury. *J Neurosci* 28:7231–7243.
27. Caro JF, et al. (1996) Decreased cerebrospinal-fluid/serum leptin ratio in obesity: A possible mechanism for leptin resistance. *Lancet* 348:159–161.
28. Wallingford N, et al. (2009) Prolylcarboxypeptidase regulates food intake by inactivating α-MSH in rodents. *J Clin Invest* 119:2291–2303.
29. Kleinridders A, et al. (2009) MyD88 signaling in the CNS is required for development of fatty acid–induced leptin resistance and diet-induced obesity. *Cell Metab* 10: 249–259.
30. Belgardt BF, et al. (2010) Hypothalamic and pituitary c-Jun N-terminal kinase 1 signaling coordinately regulates glucose metabolism. *Proc Natl Acad Sci USA* 107: 6028–6033.
31. Bouret SG, Draper SJ, Simerly RB (2004) Trophic action of leptin on hypothalamic neurons that regulate feeding. *Science* 304:108–110.
32. Horvath TL, Bruning JC (2006) Developmental programming of the hypothalamus: A matter of fat. *Nat Med* 12:52–53.
33. Plagemann A (2006) Perinatal nutrition and hormone-dependent programming of food intake. *Horm Res* 65(Suppl 3):83–89.
34. Barker DJ (2007) Obesity and early life. *Obes Rev* 8(Suppl 1):45–49.
35. Bouret SG, et al. (2008) Hypothalamic neural projections are permanently disrupted in diet-induced obese rats. *Cell Metab* 7:179–185.